

CGN: A Capacity-Guaranteed Network Architecture for Future Ultra-Dense Wireless Systems

Chaowen Deng[†], Lu Yang[‡] ✉, Hao Wu[†], Dmitry Zaporozhets[§], Miaomiao Dong[‡] and Bo Bai[‡]

[†]Department of Mathematical Sciences, Tsinghua University, Beijing, China

[‡]Theory Lab, Central Research Institute, 2012 Labs, Huawei Technology Co. Ltd.

[§]Steklov Mathematical Institute of Russian Academy of Sciences, St. Petersburg, Russia

Email: dcw21@mails.tsinghua.edu.cn, yanglu87@huawei.com, hwu@tsinghua.edu.cn, zap1979@gmail.com, dong.miaomiao@huawei.com, baibo8@huawei.com

Abstract—The sixth generation (6G) era is envisioned to be a fully intelligent and autonomous era, with physical and digital lifestyles merged together. Future wireless network architectures should provide a solid support for such new lifestyles. A key problem thus arises that what kind of network architectures are suitable for 6G. In this paper, we propose a capacity-guaranteed network (CGN) architecture, which provides high capacity for wireless devices densely distributed everywhere, and ensures a superior scalability with low signaling overhead and computation complexity simultaneously. Our theorem proves that the essence of a CGN architecture is to decompose the whole network into non-overlapping clusters with equal cluster sum capacity. Simulation results reveal that in terms of the minimum cluster sum capacity, the proposed CGN can achieve at least 30% performance gain compared with existing base station clustering (BS-clustering) architectures. In addition, our theorem is sufficiently general and can be applied for networks with different distributions of BSs and users.

Index Terms—Future wireless network architecture, cluster sum capacity, clustering

I. INTRODUCTION

The 6G era is envisioned to revolutionize wireless services via the Internet of Things (IoT) towards the future of fully intelligent and autonomous systems [1]. Unquestionably, with the future commercialization of 6G, our lifestyles will be greatly changed. More and more intelligent and digital services will emerge, such as robotic surgery, human-machine communications, blockchain-based production, satellite-unmanned aerial vehicles communications, etc. These services will accelerate the fusion of human, physical and digital worlds, but will also induce the explosive increase of the wireless data traffic. These phenomena will bring about extremely high pressure on the network architecture side, since it should not only satisfy the ever-growing requirement of the wireless data traffic, but also guarantee high-quality services for all the wireless devices densely located everywhere. Then an important problem arises: whether existing network architectures are still suitable for the 6G era?

The cellular network is the most classic architecture [2]. It is composed of cells, where each cell corresponds to the coverage area of a single base station (BS). This architecture is designed based on the BS-side information, and thus can be regarded as a BS-centric architecture [3]. The main bottleneck of the cellular architecture is the cell-edge problem, which refers to

that users located at the cell edges suffer from serious inter-cell interference [4]. Another BS-centric architecture is the BS-clustering architecture [3], where several closely-located BSs form a cluster to serve users jointly, through techniques like coordinated multipoint transmissions and receptions. However, there are still users suffering from the cluster-edge problem.

In order to eliminate the cell/cluster-edge problems in BS-centric architectures, the user-centric manner was proposed in [5], [6]. Each user autonomously chooses nearby BSs to form its own cell, called a virtual cell. These virtual cells are overlapped with each other with a high probability. One common way to deal with the overlapping cells is to merge them. Thus, large clusters exist in such user-centric architectures, where the signaling overhead and the measurement complexity are very high.

Another existing architecture is the cell-free massive multiple-input multiple-output (MIMO) [7], where all the BSs are interconnected through backhaul links to serve all the users jointly with one or several central processing units (CPUs). There are no cells and thus no cell boundaries. The main bottleneck of this architecture is its unscalability [8], since the induced signaling overhead over the backhaul links and the computation complexity at the CPUs expand much more faster than the increase of BSs and users. Actually, the number of coordinated BSs is always limited in real-world deployments. As analyzed above, existing architectures are not suitable for future ultra-dense wireless networks.

In this paper, we start from an analytical point of view and propose a brand-new architecture, called the *Capacity-Guaranteed Network* (CGN) architecture. CGN architectures can guarantee the users densely-distributed everywhere with a sufficiently high quality of service (QoS), and ensure the low signaling overhead and computation complexity simultaneously. On one hand, to realize the high QoS everywhere and mitigate the cell-edge problem, we adopt the design principle of maximizing the minimum cluster sum capacity, which will be elaborated later in Section II-B. On the other hand, to ensure that our CGN architecture is scalable with low signaling overhead, we decompose the whole network into non-overlapping clusters with each cluster operating independently [9], where the number of coordinated BSs is limited, and thus the signaling overhead and the computation

complexity are constrained by the cluster size. Therefore, the CGN architecture can realize both high capacity and high scalability simultaneously, and thus is more suitable for future ultra-dense wireless systems. We illustrate a CGN diagram in Fig. 1.

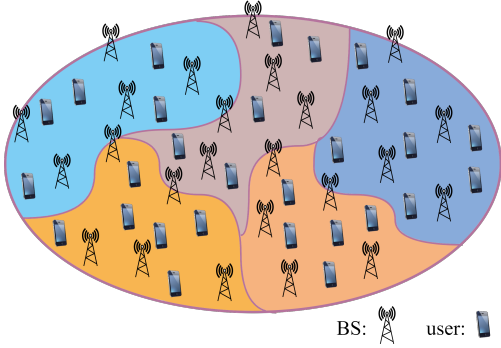


Fig. 1. A CGN architecture diagram. An ultra-dense wireless system is decomposed into non-overlapping clusters according to the principle of maximizing the minimum cluster sum capacity.

II. SYSTEM MODEL AND PROBLEM FORMULATION

A. System Model

Consider an ultra-dense wireless network consisting of M single-antenna BSs¹ and K single-antenna users [7], [10]. To capture the ultra-dense property of 6G, we assume both K and M approaching positive infinity [9]. Denote the set of BSs as $\mathcal{B} = \{b_1, \dots, b_M\}$, and the set of users as $\mathcal{U} = \{u_1, \dots, u_K\}$. Assume the network is decomposed into L non-overlapping clusters, with each cluster operating independently. The set of network nodes (BSs and users) of the l -th ($l = 1, 2, \dots, L$) cluster is denoted by \mathcal{S}_l , and $\Theta = \{\mathcal{S}_1, \mathcal{S}_2, \dots, \mathcal{S}_L\}$ forms a partition of the set $\mathcal{B} \cup \mathcal{U}$. In \mathcal{S}_l , the number of users is K_l , and the number of BSs is M_l . Thus, $K = \sum_{l=1}^L K_l$ and $M = \sum_{l=1}^L M_l$.

The channel gain between the user $u_k \in \mathcal{U}$ and the BS $b_m \in \mathcal{B}$ is denoted by h_{mk} , which is modeled as:

$$h_{mk} = \beta_{mk} \gamma_{mk}, \quad (1)$$

where γ_{mk} is the small-scale fading, following the complex Gaussian distribution $\mathcal{CN}(0, 1)$; β_{mk} represents the large-scale fading, defined as

$$\beta_{mk} = \begin{cases} d_{mk}^{-\frac{\alpha}{2}}, & d_{mk} > d_0, \\ d_0^{-\frac{\alpha}{2}}, & d_{mk} \leq d_0, \end{cases} \quad (2)$$

where d_{mk} is the Euclidean distance between b_m and u_k , α is the path-loss factor, and d_0 is a distance threshold, which is used to avoid β_{mk} approaching infinity when b_m and u_k located extremely close. Assume each user transmits with power P , and the background noise power is N_0 .

¹For distributed antenna systems, we consider M single-antenna access points (APs), instead of BSs.

B. Problem Formulation

Our objective is to design a novel wireless network architecture which not only ensures the scalability of the system, but also guarantees high communication quality everywhere. To realize the high scalability with low signaling and computational overhead, we decompose the whole system into L ($L > 1$) non-overlapping clusters. To guarantee the high communication quality, we choose the principle of maximizing the minimum cluster sum capacity. Such an objective can be formulated as

$$\mathcal{P}1: \max_{\Theta} \min_{l \in \{1, 2, \dots, L\}} C_l,$$

where C_l is the uplink sum capacity of the l -th cluster.

In order to solve $\mathcal{P}1$, the expression of C_l should be determined at first. In this paper, we focus on the uplink case. The uplink sum capacity of the l -th cluster can be determined according to [2] as

$$C_l = \mathbb{E} [\log \det (\mathbf{I}_{M_l} + P (N_0 \mathbf{I}_{M_l} + P \mathbf{\Pi}_l \mathbf{\Pi}_l^H)^{-1} \mathbf{H}_l \mathbf{H}_l^H)], \quad (3)$$

where $\mathbf{H}_l \in \mathbb{C}^{M_l \times K_l}$ and $\mathbf{\Pi}_l \in \mathbb{C}^{M_l \times (K - K_l)}$ denote the channel gain matrix and the interference matrix of the l -th cluster, respectively. Specifically, the (m, l) -th entry of \mathbf{H}_l can be determined according to (1), with $b_m \in \mathcal{S}_l$, and $u_k \in \mathcal{S}_l$. The entries of $\mathbf{\Pi}_l$ can be determined based on (1) as well, but with $b_m \in \mathcal{S}_l$ and $u_k \in \mathcal{U} \setminus \mathcal{S}_l^2$. The term $P (N_0 \mathbf{I}_{M_l} + P \mathbf{\Pi}_l \mathbf{\Pi}_l^H)^{-1} \mathbf{H}_l \mathbf{H}_l^H$ represents the signal to the interference plus noise ratio (SINR) of the l -th cluster. The asymptotic property of $\mathbf{\Pi}_l \mathbf{\Pi}_l^H = (\pi_{ij})_{M_l \times M_l}$ is shown in Lemma 1.

Lemma 1: As $K - K_l \rightarrow \infty$, $\mathbf{\Pi}_l \mathbf{\Pi}_l^H \in \mathbb{C}^{M_l \times M_l}$ converges to a diagonal matrix, which is

$$\mathbf{\Pi}_l \mathbf{\Pi}_l^H = \text{diag}(\pi_{11}, \dots, \pi_{mm}, \dots, \pi_{M_l M_l}), \quad (4)$$

whose m -th diagonal entry is

$$\pi_{mm} = \sum_{u_k \in \mathcal{U} \setminus \mathcal{S}_l} \beta_{mk}^2, \quad (5)$$

Proof: First, we prove the off-diagonal entries of $\mathbf{\Pi}_l \mathbf{\Pi}_l^H$ approaching zero as $K - K_l \rightarrow \infty$. Based on the definition of $\mathbf{\Pi}_l$, we can obtain the (i, j) -th entry ($i \neq j$) of $\mathbf{\Pi}_l \mathbf{\Pi}_l^H$ as

$$\pi_{ij} = \sum_{u_k \in \mathcal{U} \setminus \mathcal{S}_l} (\beta_{ik} \gamma_{ik}) (\overline{\beta_{jk} \gamma_{jk}}). \quad (6)$$

Since γ_{ik} is a $\mathcal{CN}(0, 1)$ random variable (RV), we let $\gamma_{ik} = a_{ik} + \mathbf{i}b_{ik}$. Both a_{ik} and b_{ik} are identically distributed real Gaussian RVs following $\mathcal{N}(0, \frac{1}{2})$. Then, (6) can be written as

$$\pi_{ij} = \sum_{u_k \in \mathcal{U} \setminus \mathcal{S}_l} \beta_{ik} \beta_{jk} [a_{ik} a_{jk} + b_{ik} b_{jk} + \mathbf{i}(a_{jk} b_{ik} - a_{ik} b_{jk})]. \quad (7)$$

Note that the product of two independent real Gaussian RVs is also a real Gaussian RV. According to Chebyshev's theorem³,

² $\mathcal{U} \setminus \mathcal{S}_l$ denotes the set of users in \mathcal{U} but not in \mathcal{S}_l .

³Chebyshev's theorem: If $\{X_i\}, i = 1, \dots, n$, are independent RVs with $E\{X_i\} = \mu_i$ and $\text{Var}\{X_i\} \leq c < +\infty$, then $\frac{1}{n} \sum_{i=1}^n X_i - \frac{1}{n} \sum_{i=1}^n \mu_i \xrightarrow{P} 0$.

(7) approaches zero as $K - K_l \rightarrow \infty$, so the off-diagonal entries of $\mathbf{\Pi}_l \mathbf{\Pi}_l^H$ approach zero.

Next, let's study the diagonal entries of $\mathbf{\Pi}_l \mathbf{\Pi}_l^H$. Similar to the above procedures, the m -th diagonal entry can be derived as

$$\pi_{mm} = \sum_{u_k \in \mathcal{U} \setminus \mathcal{S}_l} \beta_{mk}^2 (a_{mk}^2 + b_{mk}^2), \quad (8)$$

where $(\sqrt{2}a_{mk})^2 + (\sqrt{2}b_{mk})^2 \sim \chi^2(2)$ (chi-square distribution). According to Chebyshev's theorem, we can obtain (5) from (8).

The proof is completed. \blacksquare

Based on Lemma 1, (3) can be written as

$$C_l = \mathbb{E} [\log \det (\mathbf{I}_{M_l} + P \mathbf{D}_l^{-1} \mathbf{H}_l \mathbf{H}_l^H)], \quad (9)$$

where $\mathbf{D}_l = N_0 \mathbf{I}_{M_l} + P \mathbf{\Pi}_l \mathbf{\Pi}_l^H$ is a diagonal matrix. We will use (9) for cluster sum capacity calculation in section IV.

III. CGN ARCHITECTURE THEOREM

In this section, we will elaborate the core mathematical principles of CGN architectures. The theorem which gives the solution of $\mathcal{P}1$ and reveals the essence of future network architecture designs is given below.

Theorem 1: *In ultra-dense scenario, the optimal network decomposition can be achieved only if all the clusters have the same cluster sum capacity, which is:*

$$C_1 = C_2 = \dots = C_L, \quad (10)$$

Proof: We utilize the method of proof by contradiction. With a slight abuse of notation, here we denote the optimal network decomposition as Θ . It means the minimum cluster sum capacity in Θ is the maximum one among all the network decompositions.

If (10) does not hold in Θ , there exists a minimum cluster sum capacity in Θ , denoted as C_{min} . Let Θ_{min} be the set of clusters whose sum capacity equal to C_{min} . Let $|\Theta_{min}|$ denote the cardinality of Θ_{min} .

Case 1: $|\Theta_{min}| = 1$. It means there is only one cluster with the capacity of C_{min} . Assume this cluster is \mathcal{S}_i . Then we have $\Theta_{min} = \{\mathcal{S}_i\}$, and $C_i = C_{min} < C_l, (l \neq i)$. Denote $C_j = \min_{l \neq i} \{C_l\}$, and thus

$$\varepsilon = C_j - C_i > 0. \quad (11)$$

Let's consider a new decomposition generated from Θ as Θ^* , where C_i increases by an increment $\frac{\varepsilon}{3}$ and the reduction of the cluster sum capacity of other clusters will not exceed $\frac{\varepsilon}{3}$:

$$\begin{cases} C_i^* = C_i + \frac{\varepsilon}{3}, \\ C_l^* \geq C_l - \frac{\varepsilon}{3}, (l \neq i). \end{cases} \quad (12)$$

Thus C_i^* is the minimum cluster sum capacity in Θ^* . However, $C_i^* > C_i$, which means Θ is not the optimal decomposition with the maximized C_{min} . This leads to a contradiction with the original assumption that Θ is the optimal decomposition.

Case 2: $|\Theta_{min}| = n$ ($2 \leq n < L$)⁴. It means there are multiple clusters with the capacity of C_{min} . Then we have

$$\begin{cases} C_i = C_{min}, \forall \mathcal{S}_i \in \Theta_{min} \\ C_i < C_l, \forall \mathcal{S}_l \in \Theta \setminus \Theta_{min}. \end{cases} \quad (13)$$

We randomly select a cluster from Θ_{min} , might as well take \mathcal{S}_i . Denote $C_j = \min_{\mathcal{S}_l \in \Theta \setminus \Theta_{min}} \{C_l\}$, and thus

$$\varepsilon = C_j - C_i > 0. \quad (14)$$

Using the same argument as *Case 1*, we have the following relationships in Θ^* :

$$\begin{cases} C_i^* = C_i + \frac{\varepsilon}{3}, \\ C_l^* \geq C_l - \frac{\varepsilon}{3}, \forall \mathcal{S}_l \in \Theta \setminus \Theta_{min}. \end{cases} \quad (15)$$

For the cluster with C_{min} in Θ^* , there exist three possibilities:

- (i) There is a single cluster belonging to $\Theta_{min} \setminus \{\mathcal{S}_i\}$ with its capacity dropped the most, which means $|\Theta_{min}^*| = 1$. We can use the same procedures to get the contradiction as shown in *Case 1*.
- (ii) There are more than one clusters in the set $\Theta_{min} \setminus \{\mathcal{S}_i\}$ with the capacity decreased by a same value. Then the situation becomes $1 < |\Theta_{min}^*| \leq n - 1$. We can repeat the procedures from the initialization of *Case 2* until the contradiction happens.
- (iii) None of the clusters in $\Theta_{min} \setminus \{\mathcal{S}_i\}$ with the capacity changed. It means there are cluster(s) in $\Theta \setminus \Theta_{min}$ with capacity decreased, and thus $|\Theta_{min}^*| = n - 1$. We can then repeat the procedures from the initialization of *Case 2* until the contradiction happens.

The proof is completed. \blacksquare

Theorem 1 gives the optimal solution of $\mathcal{P}1$, and reveals that the optimal network architecture must satisfy the condition of equal cluster sum capacity, i.e., $C_1 = C_2 = \dots = C_L$. This is the essence of our CGN architectures. As such, our CGN can be regarded as a capacity-centric architecture, which is designed based on the information from the BS side and the user side jointly. As a contrast, conventional cellular and BS-clustering architectures are BS-centric only, missing the important information from the user side.

A key point we want to emphasize is that Theorem 1 does not impose any restrictions on the network area and the distributions of BSs and users. The only constraint is the ultra-dense scenario, which is obviously satisfied in the future 6G era aiming to connect everything. Therefore, we claim that Theorem 1 and our CGN architecture have superior generality and a wide range of applications. They are feasible for various wireless networks with different distributions of BSs and users. Besides, the number of clusters L is adaptive to concrete network requirements. If the BS coordination can not be performed in a certain network, we can set $L = M$, where the number of clusters equals to the number of BSs. Then an extreme case of CGN arises, which is equivalent to the cellular architecture.

⁴If $n = L$, the equation $C_1 = C_2 = \dots = C_L$ holds directly.

IV. ARCHITECTURE VISUALIZATION AND PERFORMANCE EVALUATION

In this section, we will visualize our proposed CGN architecture through a heuristic algorithm, and show the performance comparison across CGN, BS-clustering and cellular architectures through simulations.

A. Heuristic CGN Architecture Algorithm

Denote the cluster with the maximum cluster sum capacity C_{max} as \mathcal{S}_{max} and the cluster with the minimum cluster sum capacity C_{min} as \mathcal{S}_{min} . Based on our Theorem 1, we propose a heuristic algorithm with the objective to realize a network decomposition with $C_{max} - C_{min} \rightarrow 0$. Details are shown in Algorithm 1, where *center* denotes an $L \times 2$ matrix with each row vector representing the centroid coordinates of each cluster, *idx* denotes a $(K + M) \times 1$ vector with each entry representing the index of the clusters that a BS/user belongs to, $center_{\mathcal{S}_{max}}$ denotes the centroid coordinates of \mathcal{S}_{max} . Define $d(p, \mathcal{S}) = \min_{q \in \mathcal{S}} d(p, q)$ as the minimum Euclidean distance between the point p and the point $q \in \mathcal{S}$.

Algorithm 1 Heuristic CGN Architecture Algorithm

Input: Coordinates of users and BSs, K , M , L , and δ .

Output: *center*, *idx* and $C_l (l = 1, 2, \dots, L)$.

```

1: Initialization: Decompose the whole network into  $L$ 
   clusters based on  $k$ -means++ algorithm.
2: Compute  $C_l (l = 1, 2, \dots, L)$  based on (9) and find  $C_{max}$ 
   and  $C_{min}$ .
3: while  $C_{max} - C_{min} > \delta$  do
4:   for  $p \in (\mathcal{B} \cup \mathcal{U}) \setminus \mathcal{S}_{min}$  do
5:     if  $p = \arg \min_{p^* \in (\mathcal{B} \cup \mathcal{U}) \setminus \mathcal{S}_{min}} d(p^*, \mathcal{S}_{min})$  then
6:       Let  $p \in \mathcal{S}_{min}$ .
7:     end if
8:   end for
9:   for  $q \in \mathcal{S}_{max}$  do
10:     $center_{\mathcal{S}_{max}} \leftarrow$  the centroid coordinate of  $\mathcal{S}_{max}$ 
11:    if  $q = \arg \max_{q^* \in \mathcal{S}_{max}} d(q^*, center_{\mathcal{S}_{max}})$  then
12:      Find  $\mathcal{S}_q = \arg \min_{\mathcal{S} \neq \mathcal{S}_{max}} d(q, \mathcal{S})$ .
13:      Let  $q \in \mathcal{S}_q$ .
14:    end if
15:   end for
16:   Update center and idx.
17:   Update  $C_{max}$  and  $C_{min}$ .
18: end while
19: return center, idx and  $C_l (l = 1, 2, \dots, L)$ 

```

B. Architecture Visualization

We now demonstrate the BS-clustering and the CGN architectures. Simulation settings are shown in Table I. Assume both BSs and users are distributed in the network area with the inconstant density⁵. Here, we choose Gaussian distribution

⁵For visualization, we plot networks with fewer number of nodes in order to clearly show the architectures.

(GD) as an example, to mimic the city with denser network nodes in the central part while sparser network nodes in the marginal area. Specifically, both users and BSs are distributed according to $\mathcal{CN}(0, 1)$. BS-clustering architecture is generated by decomposing all the BSs into L non-overlapping clusters according to k -means++ algorithm. CGN is generated according to our Algorithm 1. We plot CGN and BS-clustering architectures with $K > M$ in Fig. 2. To unfold the generality of our CGN, we plot another case with $K < M$ in Fig. 3.

TABLE I
SIMULATION SETTINGS

Definition and Symbol	Value
The number of clusters (L)	40
Power constraint (P)	1 W
Noise power (N_0)	0.09 W
Path loss factor (α)	4
Distance threshold (d_0)	5 m
Capacity difference threshold (δ)	0.2 bps

In Fig. 2 and Fig. 3, BSs and users are represented by triangles and circles, respectively. A cluster is represented by network nodes interconnected with lines using the same color. Different colored areas correspond to different clusters. It can be observed in Fig. 2(a) and Fig. 3(a) that there are many clusters with BSs only, leading to a waste of resource and energy. Such phenomenon happens in BS-clustering architectures, no matter $K > M$ or $K < M$. In Fig. 2(b) and Fig. 3(b), according to the CGN architecture, this phenomenon can be totally avoided, since the CGN is designed based on the cluster sum capacity, which are determined by BSs and users jointly. To give a more in-depth analysis on the differences between BS-clustering and CGN architectures, we select several representative clusters to elaborate:

- (i) The clusters with larger sum capacity in the BS-clustering architecture will become clusters with medium sum capacity in the CGN architecture, marked as cluster A in Fig. 2 and Fig. 3. In Fig. 2(a), the sum capacity of cluster A is 0.25 bps, while is 0.16 bps in Fig. 2(b), closer to the average cluster sum capacity 0.07 bps. Similarly, the sum capacity of cluster A is 0.26 bps in Fig. 3(a) while is 0.2 bps in Fig. 3(b).
- (ii) On the contrary, some clusters with smaller sum capacity in the BS-clustering architecture will be merged and reorganized into clusters with larger sum capacity in the CGN architecture, such as cluster B in Fig. 2 and Fig. 3. In both Fig. 2(a) and Fig. 3(a), there is only one BS serving multiple users in cluster B, leading to the sum capacity of cluster B is only 1.6×10^{-6} bps in Fig. 2(a), and is 7.0×10^{-7} bps in Fig. 3(a). In the CGN architecture, cluster B contains more BSs and users. The sum capacity of cluster B becomes 2.2×10^{-4} bps in Fig. 2(b) and becomes 1.5×10^{-5} bps in Fig. 3(b).
- (iii) In the BS-clustering architecture, there exist clusters without users, such as cluster C. This is one of the shortcomings of the BS-clustering architecture: it is impossible to prevent the existence of clusters with only one kind of network nodes. The CGN network architecture can perfectly avoid this problem. It makes the sum capacity

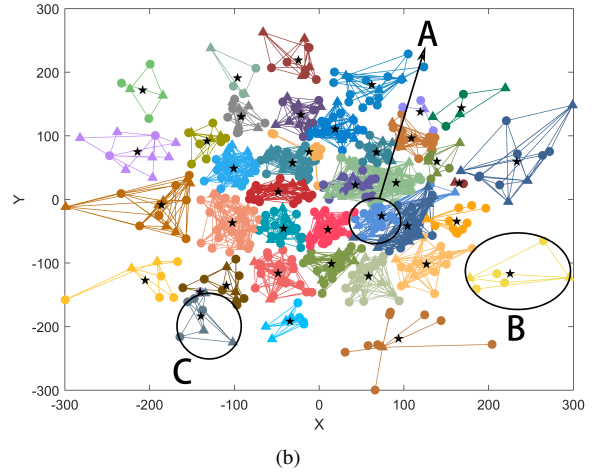
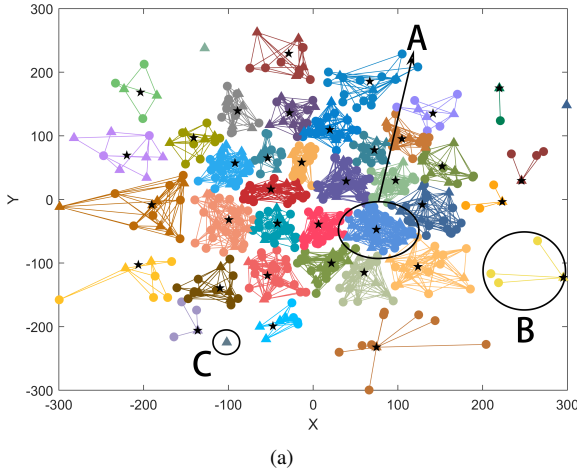


Fig. 2. Visualization of BS-clustering and CGN architectures, with $K > M$. $K = 400, M = 200$. Both BSs and users are distributed according to GD. Triangles represent BSs, circles represent users, and stars represent the centroids of clusters. (a) BS-clustering. (b) CGN.

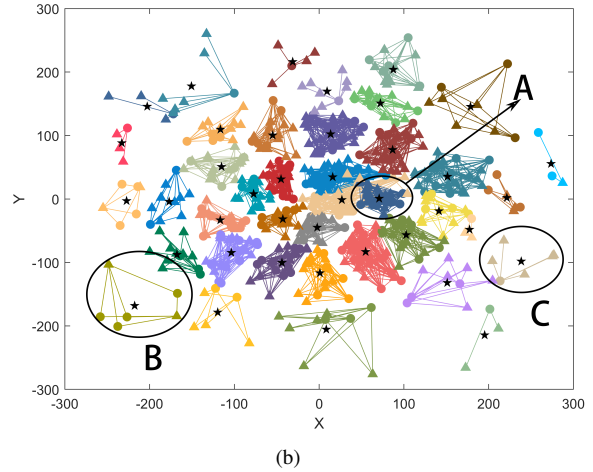
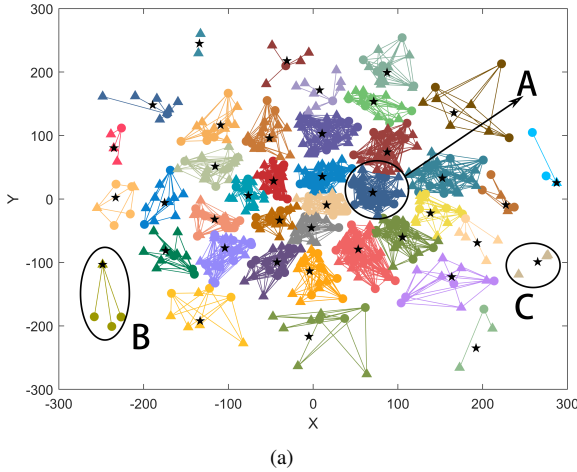


Fig. 3. Visualization of BS-clustering and CGN architectures, with $K < M$. $K = 200, M = 400$. Both BSs and users are distributed according to GD. Triangles represent BSs, circles represent users, and stars represent the centroids of clusters. (a) BS-clustering. (b) CGN.

of all clusters as equal as possible, both BSs and users should exist in all the clusters. Obviously, in Fig. 2(a) and in Fig. 3(a), the sum capacity of cluster C is 0. In Fig. 2(b) and Fig. 3(b), the cluster sum capacity become 3.8×10^{-5} bps and 2.4×10^{-5} bps, respectively.

C. Performance Comparison

In this subsection, we compare the performance across CGN, BS-clustering and cellular architectures. Unlike the choose of fewer nodes for visualization, now we adopt ultra-dense network nodes for accuracy. In simulation, we consider a square network area with side length a . Denote $K = \rho_u a^2$ and $M = \rho_b a^2$, where ρ_u and ρ_b are the density of users and BSs, respectively. Two kinds of distributions of network nodes are considered: the uniform distribution (UD) and the GD.

The variances of the cluster sum capacity C_{var} of the CGN architecture and the BS-clustering architecture are shown in Fig. 4. It can be observed that C_{var} of the CGN architecture is smaller. Especially in the UD case, C_{var} of CGN decreased by at least 30.4% compared to C_{var} of BS-clustering. It means

the CGN architecture can guarantee a more fair QoS for all the users, which is consistent with our Theorem 1.

The minimum cluster sum capacity C_{min} of three architectures are plotted in Fig. 5(a). It can be observed that C_{min} of the CGN architecture is the highest, independent of the network areas and the distributions of network nodes. Compared to the BS-clustering architecture, C_{min} of the CGN architecture with UD has at least 30% performance gain, while with GD, such performance gain can achieve at least 100 times. This is because in the BS-clustering architecture, there always exist clusters with extremely small number of network nodes, leading to the extremely low cluster sum capacity, as illustrated in Fig. 2(a) and Fig. 3(a). As for the cellular architecture, C_{min} is always zero (i.e., the lowest), corresponding to the cluster containing a single BS without users.

In Fig. 5(b), we plot the average cluster sum capacity C_{avg} of three different architectures, where $C_{avg} = (\sum_{l=1}^L C_l)/L$. Compared with the cellular architecture, C_{avg} of our CGN architecture has at least 80.3 times performance gain in the

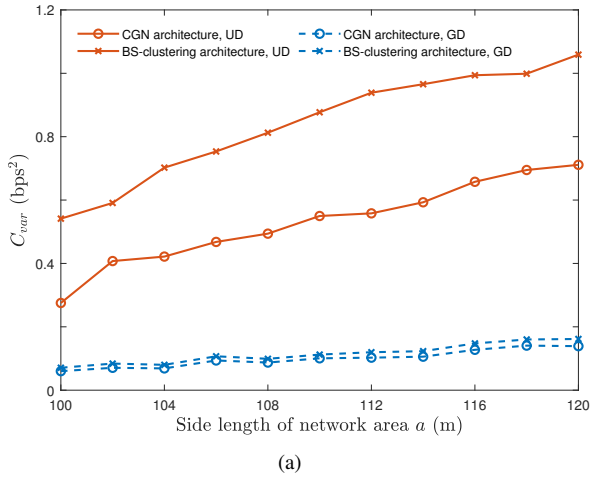


Fig. 4. Comparison between CGN and BS-clustering architectures in terms of C_{var} . Two distributions of network nodes are considered: UD and GD.

UD case, and at least 9.1 times gain in the GD case. Compared with the BS-clustering architecture, C_{avg} in our CGN has a slight reduction of 3.2% in the UD case, and 2.4% in the GD case. Combined with Fig. 5(a), it can be found that these slight degradation on C_{avg} , which can be ignored in practice, brings great performance gain on C_{min} , such as at least 100 times performance gain in the GD case and 30% performance gain in the UD case. As a brief summary, our CGN provides great performance gains on both C_{min} and C_{avg} compared with cellular architectures; it can also provide great performance gains on C_{min} compared with BS-centric clustering structures, but with a slight reduction on C_{avg} . Generally speaking, the performance of CGN is better than both BS-clustering and cellular architectures.

V. CONCLUSION

In this article, we propose a novel CGN architecture for future ultra-dense wireless systems. It guarantees high capacity and high scalability simultaneously. The design essence of CGN is summarized as our Theorem 1; the whole network should be decomposed into non-overlapping clusters with equal cluster sum capacity. Simulation results show that our CGN achieves higher capacity, which means the cell/cluster-edge problems in traditional BS-centric architectures can be alleviated greatly. Specifically, in terms of the minimum cluster capacity, our CGN outperforms BS-clustering architecture, with performance gains of at least 30%. In terms of the average capacity per BS, our CGN outperforms cellular with gains of at least 9.1 times. Our CGN also has superior scalability; the increase of network nodes in a cluster will not affect the signaling overhead and computation complexity of other clusters. More importantly, both of our theorem and CGN architecture are general enough and applicable for various scenarios with different distributions of BSs and users.

REFERENCES

[1] D. C. Nguyen, M. Ding, P. N. Pathirana, A. Seneviratne, and J. Li, "6G internet of things: A comprehensive survey," *IEEE Internet Things J.*, pp. 1–25, Aug. 2021.

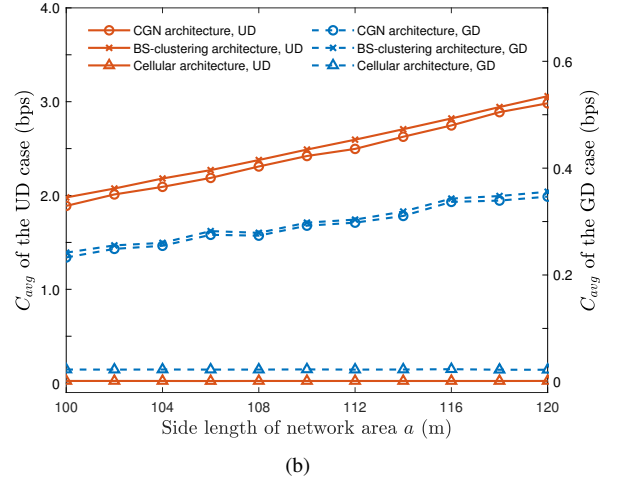
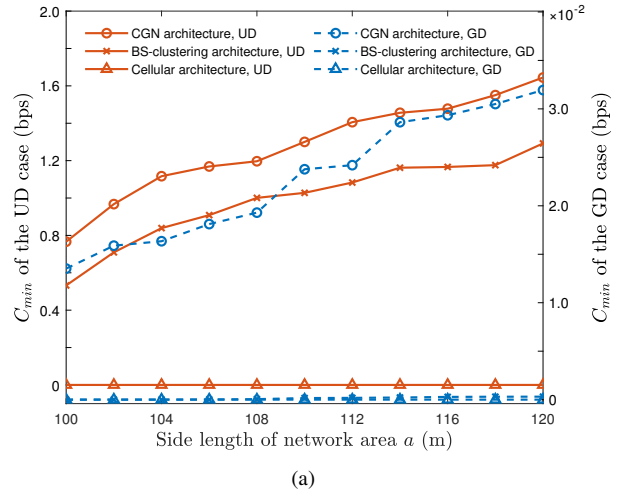


Fig. 5. Comparison across CGN, BS-clustering and cellular architectures in terms of C_{min} and C_{avg} . Two distributions of network nodes (BSs and users) are considered: UD and GD. (a) C_{min} . (b) C_{avg} .

[2] D. Tse and P. Viswanath, *Fundamentals of Wireless Communication*. United States of America by Cambridge University Press, New York, 2005.

[3] R. Sun, Y. Wang, N. Cheng, H. Zhou, and X. Shen, "QoE driven BS clustering and multicast beamforming in cache-enabled C-RANs," in *Proc. IEEE ICC*, Jul. 2018, pp. 1–6.

[4] D. Gesbert, S. Hanly, H. Huang, S. S. Shitz, O. Simeone, and W. Yu, "Multi-cell MIMO cooperative networks: A new look at interference," *IEEE J. Sel. Areas Commun.*, vol. 28, no. 9, pp. 1380–1408, Oct. 2010.

[5] Y. Zhang and Y. J. Zhang, "User-centric virtual cell design for cloud radio access networks," in *Proc. IEEE SPAWC*, Nov. 2014, pp. 249–253.

[6] C. Pan, M. Elkashlan, J. Wang, J. Yuan, and L. Hanzo, "User-centric C-RAN architecture for ultra-dense 5G networks: Challenges and methodologies," *IEEE Commun. Mag.*, vol. 56, no. 6, pp. 14–20, Jun. 2018.

[7] H. Q. Ngo, A. Ashikhmin, H. Yang, E. G. Larsson, and T. L. Marzetta, "Cell-free massive MIMO versus small cells," *IEEE Trans. Wireless Commun.*, vol. 16, no. 3, pp. 1834–1850, Jan. 2017.

[8] M. Matthaiou, O. Yurduseven, H. Q. Ngo, D. Morales-Jiménez, S. Cotton, and V. Fusco, "The road to 6G: Ten physical layer challenges for communications engineers," *IEEE Commun. Mag.*, vol. 59, pp. 64–69, Feb. 2021.

[9] L. Yang *et al.*, "What should 6G architectures be?" 2021, *arXiv: 2110.03157*. [Online]. Available: <https://arxiv.org/abs/2110.03157>

[10] G. Interdonato, H. Q. Ngo, E. G. Larsson, and P. Frenger, "How much do downlink pilots improve cell-free massive MIMO?" in *Proc. IEEE GLOBECOM*, Dec. 2016, pp. 1–7.